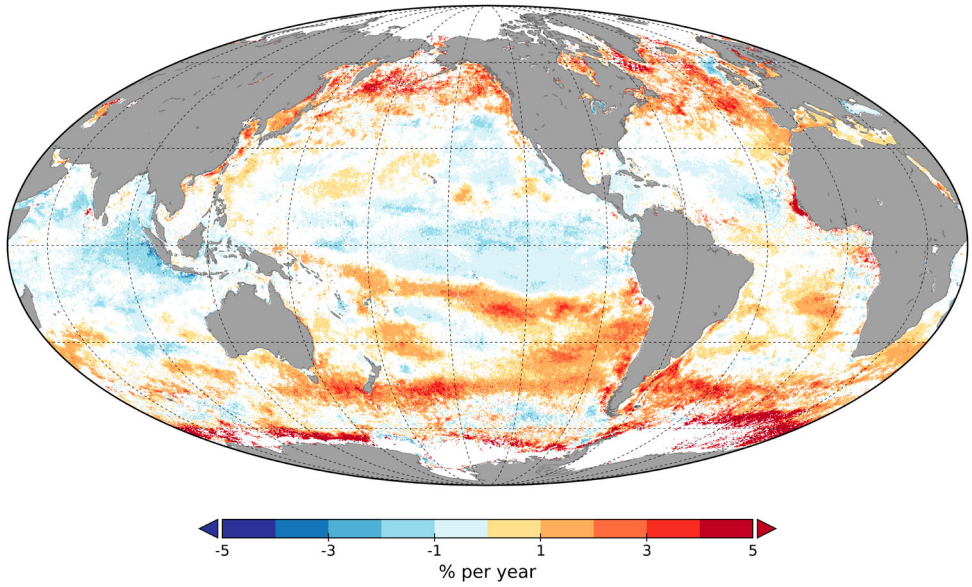

Figure 1.5.4. Global chlorophyll trend map (September 1997 to December 2016). Only statistically significant ($p < .05$) trends are shown.

South-West India. More positive anomalies appear as one moves towards the Southern Ocean, with very high positive anomalies appearing close to the Antarctic. The positive anomalies are more pronounced in the Pacific than in the Indian Ocean sector of the Southern Ocean.

The anomalies in the CMEMS regions are shown in more detail in Figure 1.5.3(b–f). The Arctic Region (Figure 1.5.3(c)) shows mostly negative anomalies except in the Atlantic sector. The anomalies in the Black Sea (Figure 1.5.3(f)) are negative, whereas those in the Mediterranean (Figure 1.5.3(d)) show an east–west divide pattern (negative in the west and positive in the east). The North-West Atlantic Region (Figure 1.5.3(b)) shows positive anomalies except for the European waters, which show mostly negative anomalies. The anomalies in the Baltic (Figure 1.5.3(e)) show pronounced regional differences, with the western part being dominated by negative anomalies, the eastern parts by positive anomalies and weak anomalies in between.

The global trends in chlorophyll concentration (Figure 1.5.4) were calculated for every 4×4 km pixel, for the entire study period (September 1997–December 2016). The trend detection method is based on the Census-I algorithm as described by Vantrepotte et al. (2009), where the time series is decomposed as a fixed seasonal cycle plus a linear trend component plus a residual component. Noting that Mélin et al. (2017) calculated trends from October 1997 to September 2015, the similarities between the two results are very consistent. We note great swaths of the tropical ocean where the trends are negative, but higher latitudes show strong positive anomalies, with the notable exception of the South Pacific subtropical gyre core. Most of the northern and tropical Indian Ocean shows negative anomalies.

1.6. Nitrates

Leading authors: Coralie Perruche, Cosimo Solidoro

Contributing authors: Stefano Salon

Statement of outcome: In this new section in chapter one of the Ocean State Report, the distribution of nitrate – a macro-nutrient limiting primary production – is studied over the 1993–2016 period. We show that its interannual variability between 40°S and 40°N strongly correlates with El Niño Southern Oscillation. During 2016, a negative anomaly emerged in equatorial Pacific due to the reduced intensity of equatorial upwelling. In the Mediterranean Sea, a negative anomaly occurred in 2016 which is possibly due to stronger water column stratification.

Products used:

Ref. no.	Product name and type	Documentation
1.6.1	GLOBAL_REANALYSIS_BIO_001_018 Reanalysis	PUM: http://marine.copernicus.eu/documents/PUM/CMEMS-GLO-PUM-001-018.pdf QUID: http://marine.copernicus.eu/documents/QUID/CMEMS-GLO-QUID-001-018.pdf

(*Continued*)

Continued.

Ref. no.	Product name and type	Documentation
1.6.2	MEDSEA_REANALYSIS_BIO_006_018 Reanalysis	PUM: http://marine.copernicus.eu/documents/PUM/CMEMS-MED-PUM-006-008.pdf QUID: http://marine.copernicus.eu/documents/QUID/CMEMS-MED-QUID-006-008.pdf

Figure 1.6.1 presents the surface concentration of nitrate computed from the CMEMS global biogeochemical reanalysis (product reference 1.6.1). The 30°S–30°N distribution is characterised by undetectably low concentrations of nitrates in sub-tropical oligotrophic gyres except in a rich tongue in the equatorial Pacific. This depletion in surface waters of oligotrophic gyres is due to a permanent stratification that induces a very limited entrainment of nitrates within the shallow well-lit mixed layer. These small amounts of nitrates are immediately utilised by phytoplankton. The nitrate tongue in tropical Pacific and along eastern boundaries coasts are induced by the equatorial and coastal upwelling (vertical velocities) of deep nitrate-rich waters. At higher latitudes, the mixed layer deepening in winter entrains large amounts of nitrates within it.

If we now consider the 2016 anomaly on Figure 1.6.2, we see a large negative anomaly which can be attributed to the 2016 El Niño event which reduces the intensity of the equatorial upwelling and the vertical supply of nitrates (Radenac et al. 2001). Nitrate-poor waters of the Western Pacific are advected eastward. The cold tongue of the tropical Pacific is referred to an HNLC region (High Nutrient/Low Chlorophyll). This low phytoplankton biomass relative to available nitrate concentrations in the euphotic layer is explained by micronutrient limitation, namely iron. This nitracline deepening during El Niño years is thus associated

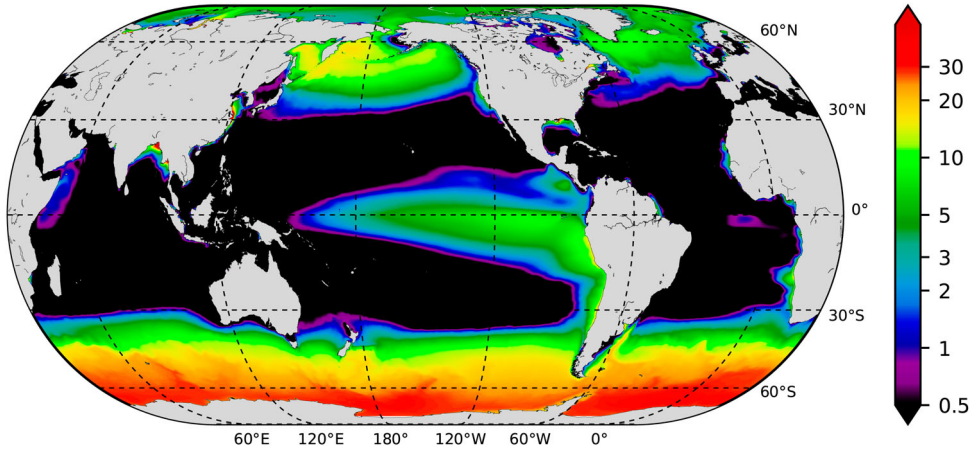

Figure 1.6.1. Map of surface nitrates (mmol/m^3) computed from the CMEMS global reanalysis product (see text for more details) over the period 1993–2014 (log scale).

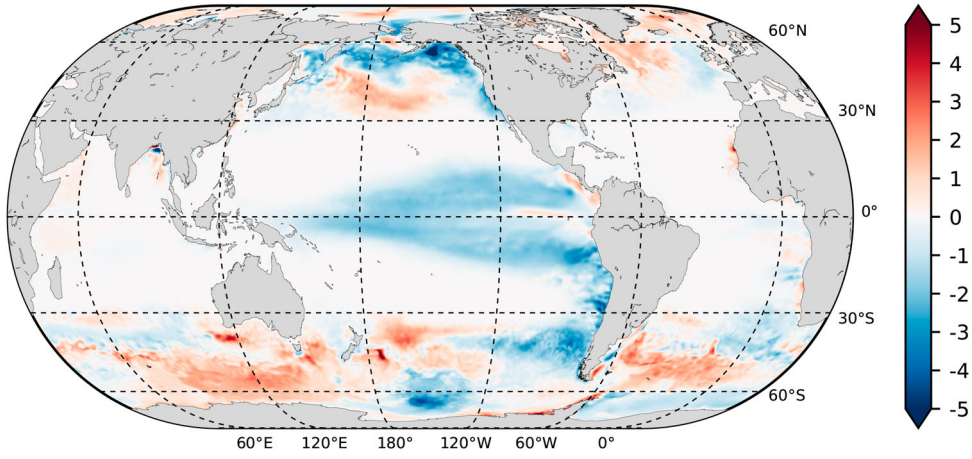

Figure 1.6.2. Anomalies of surface nitrates (mmol/m^3) in 2016 relative to climatological period 1993–2014. At each grid cell, the time series was previously detrended. Our simulation starting from WOA and GLODAP climatologies and being relatively short, we prefer removing the trend to filter the model drift.

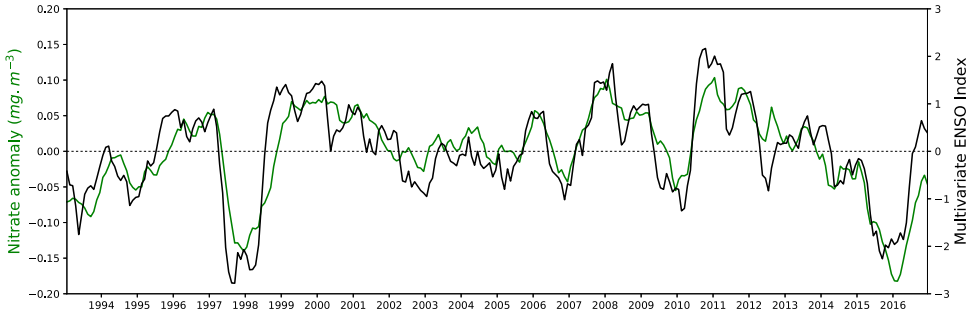

Figure 1.6.3. (Green – left axis) Surface nitrates mean over 40°S–40°N region (mmol/m^{-3}). Signal previously detrended and deseasonalised with a monthly 1993–2014 climatology. (Black – right axis) The monthly multivariate ENSO index (MEI), downloaded from the NOAA website (https://www.esrl.noaa.gov/psd/enso/mei/). Note that the sign of the ENSO index is inverted (El Niño years correspond to negative values).

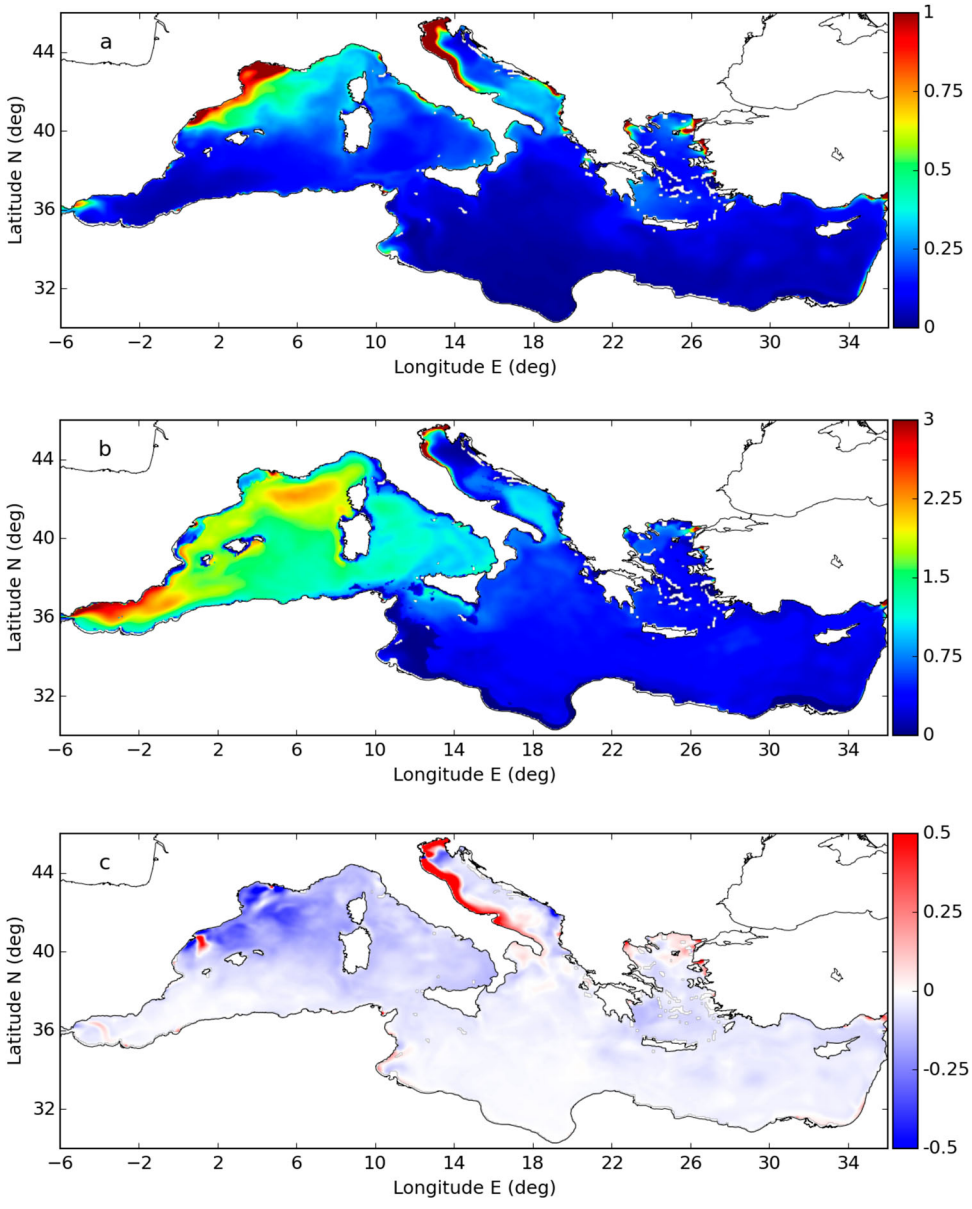

Figure 1.6.4. Surface (a) and subsurface (b, 0–150 m) maps of nitrate (mmol/m^3) computed from the CMEMS Mediterranean reanalysis product (see text for more details) over the period 2002–2014. Anomalies of surface nitrate (c, mmol/m^3) in 2016 relative to climatological period 2002–2014.

with ferricline deepening (Radenac et al. 2001; Wang et al. 2005) and with a negative anomaly of chlorophyll (see Figure 1.5.3 in Section 1.5). The time series of the nitrate anomaly (signal previously detrended and deseasonalised) over 40°S–40°N region (Figure 1.6.3) shows a strong correlation between nitrate concentration and ENSO index.

At the regional scale, other processes can play important roles in shaping nutrient distribution. As an interesting example, the Mediterranean Sea (Figure 1.6.4(a), product reference 1.6.2) shows a spatial pattern of nutrient distribution that depends on the superposition of inverse estuarine circulation of the Atlantic water inflowing from the Gibraltar Straits, local areas of upwelling (i.e. north-western Mediterranean Sea and Southern Adriatic Sea), an uneven distribution of rivers, and – most importantly – the activity of plankton autotrophs, which depletes nutrient concentration along the Atlantic modified water while enriching through their sinking the outflowing deeper waters (i.e. the clearly shown east to west gradient in the subsurface 0–150 m map, Figure 1.6.4(b)). In 2016, the anomaly map (Figure 1.6.4(c)) highlights a generally lower than average value of nitrate concentration, more evident in specific areas (e.g. north-western Mediterranean, south-eastern Tyrrhenian Sea, north-western Ionian Sea, south-eastern Aegean Sea, central Levantine), which is related to a general negative anomaly of the mixed layer depth (not shown), and therefore to a stronger water column stratification. The positive anomaly observed along the Italian coast of the Adriatic Sea is related to the 2016 phytoplankton negative anomaly, as prescribed by the assimilated ocean colour chlorophyll (Figure 1.5.3) and the climatological (i.e. constant in years) nutrient river discharge rates.

1.7. Air-to-sea carbon flux

Leading authors: Coralie Perruche, Cosimo Solidoro

Contributing authors: Gianpiero Cossarini

Statement of outcome: In this new section of the Ocean State Report, we study the sea-to-air CO_2 flux as described by a global and a regional coupled physical-biogeochemical model. At the global scale, the model simulates a relatively stable ocean carbon uptake during the 1990s and a sharp increase since the beginning of the 2000s. In the Mediterranean Sea, model results indicate that it acts as a weak sink during the last decade. In 2016, there is a strong negative anomaly of the equatorial Pacific outgassing due to a weaker upwelling (end of El Niño event).

Products used:

Ref. no.	Product name and type	Documentation
1.7.1	GLOBAL_REANALYSIS_BIO_001_018 Reanalysis	PUM: http://marine.copernicus.eu/documents/PUM/CMEMS-GLO-PUM-001-018.pdf QUID: http://marine.copernicus.eu/documents/QUID/CMEMS-GLO-QUID-001-018.pdf
1.7.2	MEDSEA_REANALYSIS_BIO_006_018 Reanalysis	PUM: http://marine.copernicus.eu/documents/PUM/CMEMS-MED-PUM-006-008.pdf QUID: http://marine.copernicus.eu/documents/QUID/CMEMS-MED-QUID-006-008.pdf

The concentration of atmospheric CO_2 has exceeded 400 ppm in 2015 and has thus increased by about 40% from about 280ppm in the pre-industrial era (Conway et al. 1994, Masarie and Tans 1995, www.esrl.noaa.gov/gmd/ccgg/trends/). This increase would have been much stronger without the contribution of the ocean and land biospheres which absorb each year roughly one half (25% ocean and 25% land) of the anthropogenic carbon emissions (Le Quéré et al. 2016, Ballantyne et al. 2012). The CO_2 flux is directly linked to the CO_2 partial pressure (pCO_2) in the ocean (product no. 1.7.1, 1.7.2) and in the atmosphere, but also to CO_2 solubility in sea water and to wind speed (Sarmiento and Gruber 2006, Takahashi et al. 2002, Wanninkhof 1992).

A few processes called 'pumps' are driving the air–sea exchange of CO_2 and the vertical distribution of carbon in the ocean. The ocean CO_2 partial pressure is prominently controlled by the physico-chemical pump of solubility which increases as temperature and salinity fall. CO_2-enriched water masses are then trapped below the thermocline where deep water convection occurs. As a consequence, the solubility pump is stronger at high latitudes. The second pump is the so-called 'organic carbon pump', which refers to biological processes that sustain a vertical downward flux of carbon (Sarmiento and Gruber 2006, Gehlen et al. 2011). Through photosynthesis, phytoplankton absorbs dissolved inorganic carbon (DIC) in the surface sunlight layer (euphotic zone) to build organic matter, which is then remineralised in the ocean interior into DIC after particle sinking. The third pump – the 'carbonate pump' – has a negative feedback on ocean carbon uptake as it counteracts the downward flux of DIC into the deep ocean (Gehlen et al. 2011). This process involves calcifiers – plankton species such as coccolithophores (phytoplankton) or foraminifera (zooplankton). To build their carbonate shell, they absorb DIC and release CO_2.